DOI: http://dx.doi.org/10.32571/ijct.1207544 **E-ISSN: 2602-277X**

International Journal of Chemistry and Technology

http://dergipark.org.tr/ijct

Research Article

Production and characterization of polyamide-6 (PA6) and cellulose acetate (CA) based nanofiber membranes by electrospinning method

Abdullah GUL[1*] Ismail TIYEK[2]

[1]*Department of Materials and Energy, Hemp Research Institute, Yozgat Bozok University, 66200, Yozgat, Türkiye*

[2]*Department of Textile Engineering, Faculty of Engineering and Architecture, Kahramanmaras Sutçu İmam University, 46050, Kahramanmaras, Türkiye*

Received: 20 November 2022; Revised: 2 June 2023; Accepted: 9 June 2023

*Corresponding author e-mail: abdullahgul46@gmail.com

Citation: Gul, A.; Tiyek, I. *Int. J. Chem. Technol.* **2023**, 7(1), 91-101.

ABSTRACT

In this study, electrospinning of Polyamide-6 (PA6)/Cellulose Acetate (CA) polymers prepared in different mixing ratios (100/0, 90/10, 80/20, 70/30, 60/40, 50/50) for nanostructured membrane production. It aims to produce nanofiber membranes with the method.

With the study, the average nanofiber diameters of the membranes were calculated. It has been determined that the average diameter of the nanofibers in the structure of the membranes produced by the electrospinning method is between 150 and 300 nm. From the characteristic peak bands obtained as a result of the FTIR analysis, it was determined that the PA6/CA structure was not deteriorated in the nanofiber material. In addition, it was determined that smooth and very fine nanofibers were formed in the materials produced from SEM images. It was observed that the conductivity of the solution decreased with the increase of the CA mixing ratio in the PA6/CA polymer solution and accordingly the fiber diameter became thinner.

Keywords: Nanofiber, membrane, electrospinning, oolyamide-6, cellulose acetate.

Elektrospinning yöntemiyle poliamid-6 (PA6) ve selüloz asetat (CA) esaslı nanofiber membranların üretimi ve karakterizasyonu

ÖZ

Bu çalışmada farklı karışım oranlarında (100/0, 90/10, 80/20, 70/30, 60/40, 50/50) hazırlanan Poliamid-6 (PA6)/Selüloz Asetat (CA) polimerlerinin elektrospinning yöntemi ile nanoyapılı membranların üretilmesi amaçlanmıştır. Çalışma ile membranların ortalama nanolif çapları hesaplanmıştır. Elektrospinning yöntemiyle üretilen membranların yapısındaki nanoliflerin ortalama çapının 150 ile 300 nm arasında olduğu tespit edilmiştir. FTIR analizi sonucunda elde edilen karakteristik pik bantlarından nanolif malzemede PA6/CA yapısının bozulmadığı belirlenmiştir. Ayrıca SEM görüntülerinden üretilen malzemelerde pürüzsüz ve çok ince nanoliflerin oluştuğu belirlenmiştir. PA6/CA polimer çözeltisinde CA karışım oranının artmasıyla çözeltinin iletkenliğinin azaldığı ve buna bağlı olarak fiber çapının inceldiği gözlenmiştir.

Anahtar Kelimeler: Nanolif, membran, elektrospinning, polyamid 6, selüloz asetat.

1.INTRODUCTION

Recently, interest in nano-sized fiber-based materials produced by electrospinning method has increased considerably due to their superior properties (large surface area relative to volume, very small pore size, flexible surface functionality, superior mechanical properties) and common application areas (filtration, composite, medical). Therefore, nano-structured fibers and nanofiber-based materials are becoming increasingly popular and important both in research and development studies and in industry.[1-5]

DOI: http://dx.doi.org/10.32571/ijct.1207544 E-ISSN: 2602-277X

Electrospinning has become a popular technique for the production of nanofibers with diameters in the range of a few microns and submicrons.[6] Electrospinning method, in which polymeric filaments are produced using electrostatic force, was patented for the first time by Formhals in 1934.[9] Unlike the conventional fiber spinning systems like melt spinning, wet spinning, dry spinning etc., the electrospinning process uses electric field force instead of mechanical force to draw and stretch a polymer jet.[7,8] When an electric field is applied to a polymer solution, the polymer solution will be charged and the charged solution drawn out of the capillary tip. The jet with small diameter will undergo stretching and bending instability. At this stage, the solvent rapidly evaporates and the polymer solution solidifies on a collector in the form of nanofibers.[10]

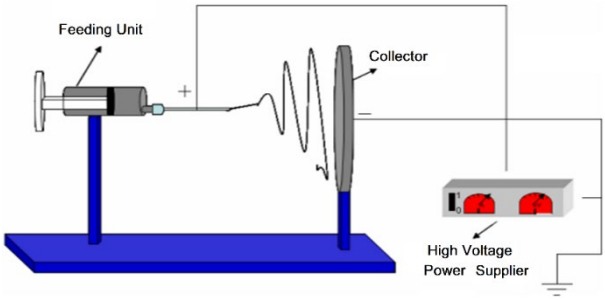

Figure 1. Basic electrospinning system.[10]

A basic electrospinning system mainly consists of a feeding unit, a highvoltage power supplier and a collector (Figure 1).[6,9] The parameters in the electrospinning process can be classified as system, solution and environmental parameters. System parameters are applied electric field, the distance between collector and needle tip, feeding rate of polymer solution, etc., solution parameters are concentration, viscosity, conductivity, surface tension, etc., and environmental parameters are climate humidity, temperature, etc. The structure and morphology of nanofibers are determined by a synergetic effect of system, solution and environmental parameters morphology. For example, finer fiber diameters are spun from smaller diameter needle tips; increasing the fluid ratio results in a larger fiber diameter; higher voltage application reduces the fiber diameter, but a beaded fiber structure emerges.[10,11]

The material properties affecting the electrospinning fiber production technique are as follows; polymer concentration, solution viscosity value, electrical conductivity of the solution and solvent of the polymer. Among the membrane material properties, the solution concentration plays an important role in keeping the nanofiber structure stable. Because it also affects the solution viscosity value, the surface tension of the solution and other characteristic properties of the solution, such as the conductivity value. The type of solvent used is another important factor. Because the solvent property affects the surface tension of the solution and the evaporation process in the electric field. Solvents with volatile properties affect the surface morphology of the fiber and the formation of a wide reticulated structure.[12,13]

PA6 (Figure 2) is a biocompatible and biodegradable synthetic polymer with good mechanical and physical properties. It is generally obtained by ring-opening polymerization of 'ε-caprolactam'. It has a very wide usage area, especially in the textile industry. Electrospinning method is preferred for the production of more robust and biocompatible nanofiber-based scaffolds in tissue engineering applications.[14]

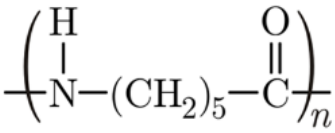

Figure 2. Chemical structure of Polyamide 6.[17]

Cellulose acetate (Figure 3) is the most important organic acid-based cellulose derivative. It is used to obtain plastic products, films and fibers. Film strips obtained from cellulose acetate can preserve their structure for a long time without deteriorating.[15] The most important features of cellulose acetate are; mechanical durability, high wear resistance, dyeability, machinability and mouldability.[16].

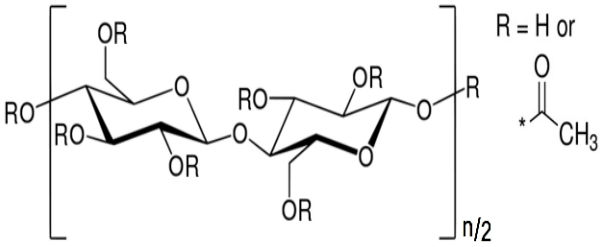

Figure 3. Chemical structure of cellulose acetate.

There has been a huge requirement for efficient water filtration technologies because of population growth, global warming, contamination of freshwater and reduction of clean water resource, and this has prompted increased attention to the development of advanced nanomaterials. Nanofibers are the latest generation of membranes, which contribute extraordinary features. The size-dependent filtration is conceivable by means of nanofiber membranes as they have superior porosity, and this pore size is adjustable through the manufacturing procedure. Consequently, it is time to thoroughly review the different nanofiber production techniques along with their benefits and drawbacks, and use of nanofiber membranes in desalination and water treatment; which will format future trends in the research of nanofiber membranes.[17]

DOI: http://dx.doi.org/10.32571/ijct.1207544 E-ISSN: 2602-277X

Membranes, which are the most important parameter of membrane-structured filtration treatment methods, act as an intermediate phase in the form of a semi-permeable barrier between two phases. Membrane processes are classified on the basis of membrane pore sizes and driving force.[18] The functions of the filtration systems and the pore sizes of the membranes are clearly shown in Figure 4.[10]

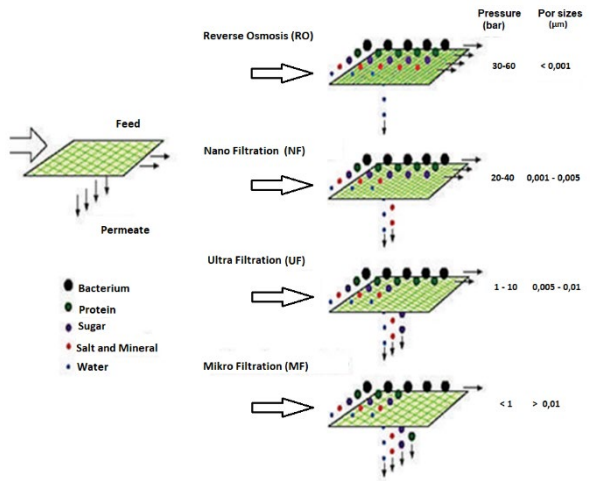

Figure 4. Identification of membranes according to their pore size and the components they capture.[13]

Polyamide 6 (PA6) was selected as a raw material because of the low-cost performance ratio. It also has good mechanical properties such as high tensile strength, flexural strength, and impact resistance. In addition, it is recyclable and has resistant to mildew and bacteria.[19-21] Being hydrophilic, cellulose acetate (CA) offers a good fouling resistance. The fouling of membranes by proteins and other biomolecules is generally attributed to the hydrophobic nature of membranes, which leads to high interfacial energy with water-rich media that is reduced upon biomolecule adsorption.[8] Many researchers have demonstrated that an increase in the hydrophilicity of membranes significantly reduces membrane fouling as a result of the reduced hydrophobic interaction between proteins and membrane surfaces.[11,22-24] In addition, CA is a potentially outstanding ultrafiltration membrane material because of the advantages such as better permeability, moderate flux, high salt rejection properties, relatively easy manufacture, cost-effectiveness, and renewable source of raw material
Through this study, the interactions of PA6 and CA polymers have been extensively studied. Analyzes of both solutions and nanofiber membrane structures were performed with different mixing ratios of PA6/CA combinations. This study focused on that the most suitable PA6/CA mixing ratio could be used in the production of nanofiber membranes.

2. MATERIALS AND METHODS

2.1. Materials

PA6 pellet (Formula Weight: 113.6 g/mol, density: 1.084 g/mL), cellulose acetate (CA) ($C_{12}H_{16}O_8$, Mn ~30,000 by GPC), formic acid (HCOOH, >98%) and acetic acid (CH_3COOH, 100%) were obtained from Sigma Aldrich.

2.2. Methods

Solutions were prepared at different mixing ratios, with a total solids content of 20% by weight. A total of 6 different solutions were prepared with these mixed ratios, the ratio of PA6/CA for each solution being 100/0, 90/10, 80/20, 70/30, 60/40 and 50/50 by weight. Formic acid and acetic acid were used as the solvent at a ratio of 1:1. Each solution was first stirred at 50 °C for 30 minutes in a magnetic stirrer with a heater, then stirred at room temperature for 12 hours. The mixed solutions were finally washed for 30 minutes, processed in an ultrasonic bath at room temperature.

Electrospinning processes were carried out on Inovenso brand NanoSpinner PilotLine model semi-industrial multi-needle electrospinning device (Figure 5), located in Kahramanmaraş Sütçü İmam University Materials Research Laboratory in USKIM. During the extraction of the mixtures from the device, parameters such as power, feeding, and needle tip-collector distance were determined with precision. The prepared polymer solutions were placed in the device after being drawn into a 10 mL plastic syringe, respectively. A 48 cm wide white spunbond nonwoven fabric with a weight of 12 g/m^2 and a polypropylene-based, calender-treated base material was used as the base material in the electrospinning device. The electrospinning parameters used in this study to obtain a smooth and continuous nanofiber membrane surface are given in Table 1.

Table 1. Electrospinning production parameters.

Feed Rate (mL/h)	Distance (mm)	Voltage (kV)	Total solid ratio (%)	Membrane ply
0,5±0,1	190	27	20	50

Viscosity values of the solutions used in the production of membrane samples were carried out in Brookfield DV-I + Viscometer device, using spindle no. 4, at room temperature, at 50 and 100 rpm, according to ISO 2555 standard, at two different rotational speeds. For the electrical conductivity analysis of the mixture solutions, it was measured separately as mV in the InoLab PH 7110 brand conductivity measuring device and as µS in the Hanna HI brand conductivity device.

In order to examine the morphological structure of the produced membrane samples, firstly, the samples were gold-plated in a Cressington 108auto gold-plating device,

DOI: http://dx.doi.org/10.32571/ijct.1207544 E-ISSN: 2602-277X

and then SEM photographs were taken with the ZEISS brand EVO / LS10 model scanning electron microscope (SEM). The average nanofiber diameters of the membrane samples were determined by making 20 measurements on the SEM images of each sample. Membrane thickness measurements were carried out for each sample in 5 different regions using a digital micrometer. Strength tests were carried out according to EN ISO 2062 standard, with 0.05 MPa prestress at 50 mm/min jaw speed and 12 cm between jaws. Three different strength tests were performed for each sample.

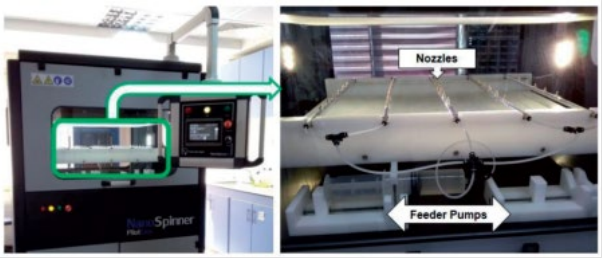

Figure 5. INOVENSO NanoSpinner PilotLine semi-industrial multi-needle electrospinning device.[18]

3. RESULTS AND DISCUSSION

For the characterization of the prepared polymer solutions, their density, electrical conductivity and viscosity were measured. The chemical and morphological structures of the nanofiber filter membrane materials produced by the electrospinning method were investigated by FTIR and SEM analyses, respectively. In addition, thickness and strength tests of nanofiber membranes were carried out.

3.1. Solution characterization studies

In this study, the effects of solution density, electrical conductivity, pH and viscosity values of prepared PA6/CA solutions on the nanofiber structures were investigated.

3.1.1. Solution density analyzes

Density studies of PA6/CA solutions prepared in different mixing ratios (100/0, 90/10, 80/20, 70/30, 60/40 and 50/50) were carried out according to TS ISO 3507 standard. The density graph of PA6/CA solutions prepared at different mixing ratios is given in Figure 6.

As seen in Figure 6, as the weight ratio of CA in the solution at different mixing ratios increases, the density values of the mixed solution also increase. This increase in density can be attributed to the increase in the ratio of CA, whose density value is higher than PA6, in the solution mixing ratio. In addition, the results obtained were found to be compatible with studies in the literature.[25]

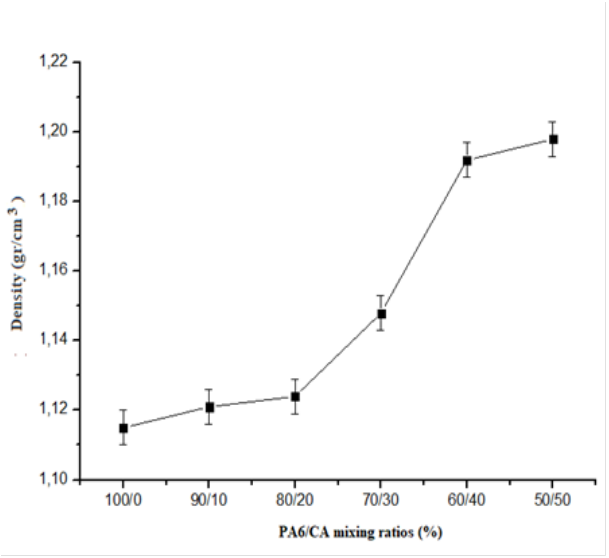

Figure 6. Density values of PA6/CA solutions at different mixing ratios.

3.1.2. Solution conductivity analyzes

Depending on the CA mixing ratios in the solution, the electrical conductivity measurement results of the mixtures are graphically given in Figure 7.

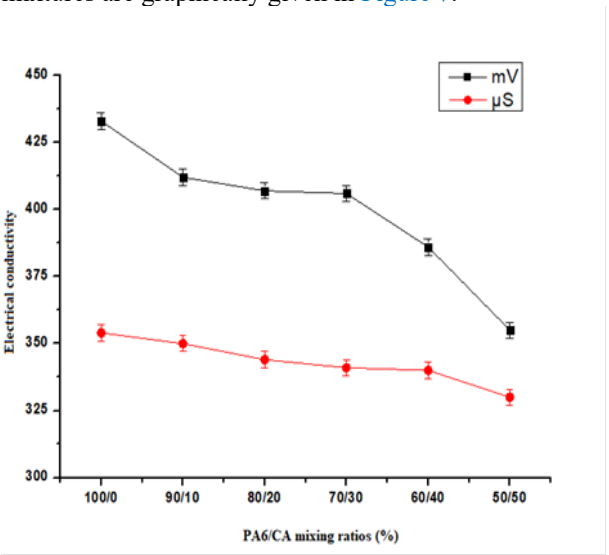

Figure 7. Effect of PA6/CA mixing ratios on the electrical conductivity µS and mV.

The electrical conductivity of the solution decreased with increasing CA in the solution mixing ratios. This decreasing electrical conductivity value directly affected the working process of the polymer solutions with the electrospinning device, and it was observed that the solution solidifications on the jet increased due to the increase in the CA ratio in the polymer mixture.[26]

3.1.3. Solution viscosity analyzes

The viscosity value graph obtained from the kinematic viscosity measurement of the polymer solutions prepared

DOI: http://dx.doi.org/10.32571/ijct.1207544 E-ISSN: 2602-277X

depending on the CA mixing ratios is given in Figure 8. For the viscosity study, the values were compared at two different speeds, 50 and 100 rpm. Viscosity results at both speeds have been found to support each other.

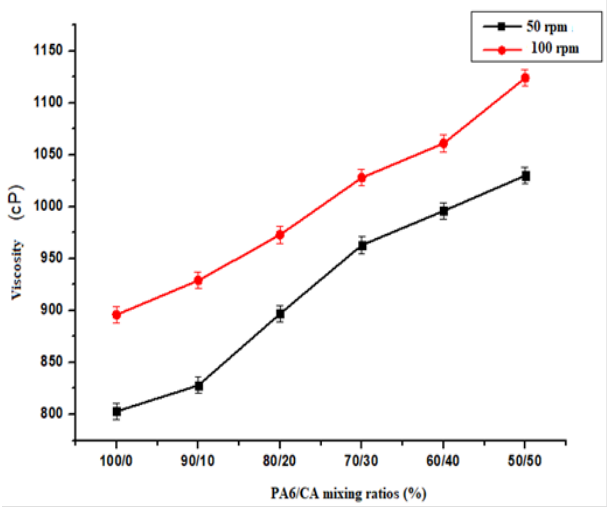

Figure 8. Viscosity value graph of PA6/CA solutions.

According to the results obtained, the viscosity value increased visibly as the CA ratio in the solution mixing ratios increased. In the studies conducted in the literature, studies supporting this result were presented.[27,28]

3.2. Membrane characterization studies

In this section, the effects on FTIR, SEM, membrane thickness and strength values on nanofiber membranes produced depending on the PA6/CA ratios in different mixing ratios obtained by the electrospinning method were investigated.

3.2.1. Fourier transform infrared (FTIR) analysis

FTIR spectra of the pure CA polymer and PA6/CA nanofiber membranes in the wavenumber range of 4000 to 450 cm^{-1} are given in Figure 9. Probable assignments for bands in the FTIR spectrum corresponding to chemical structures are described below.

The FTIR spectrum of 100 % PA6 membrane showed a peak at wavenumber of 3295 cm^{-1}which correspond to the NH bending vibration in primary amine and hydrogen-bonded NH stretching.[29,30] The band at 3095 $cm^{-1}$was assigned to NH fermi resonance. The peaks at 2933 cm^{-1} and 2856 cm^{-1} were assigned to CH_2 asymmetric and symmetric stretching vibrations, respectively.[30] The bands at 1640 cm^{-1} and 1548 cm^{-1} were assigned to C=O amide I and N–H and C–N combination amide II stretch, respectively.[30,31] The bands of CH_2 scissoring were obeserved at 1460 cm^{-1} and 1435 cm^{-1} .[35] The bands corresponding to vibration of amide III and CH_2 wag were observed at 1367 cm^{-1}, 1262 cm^{-1} and 1208 cm^{-1}.[30,33] The bands at 1170 cm^{-1} and 1118 cm^{-1} were assigned to CONH skeletal motion and CC stretching (amorphous) .[30] The bands at 975 cm^{-1} and 705 cm^{-1} were assigned to CONH in plane vibration(γ) and CH_2 rocking (amide V).[29,30,34]

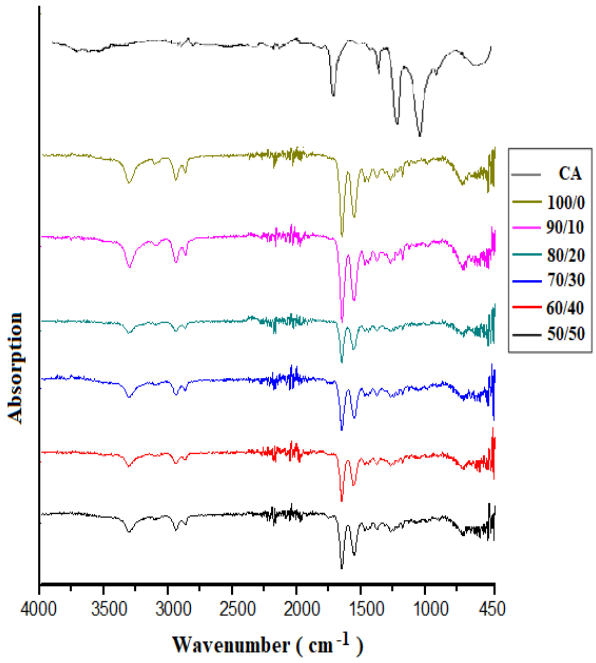

Figure 9. FTIR spectra of PA6/CA nanofiber membranes produced by electrospinning method.

The FTIR spectrum of pure CA polymer showed peaks at wavenumber of 2978 cm^{-1} and 2877 cm^{-1} corresponded to the stretching of C–H of CH_3 and CH_2, respectively.[35-37] The characteristic peaks at 1745 cm^{-1}, 1369 cm^{-1} and 1221 cm^{-1} were attributed to the C=O stretching band of the ester carbonyl group, C–H bending vibration of CH_3 in the acetyl group (CH_3–C=O) and C–O stretching of acetyl group (–O(C=O) –CH_3), respectively.[35,36,38-40] The peak at 1036 cm^{-1}were assigned to C–O–C of the cellulose backbone.[40] The peak at 897 cm^{-1} was attributed to the combined contributions from C-O stretching and CH_2 rocking vibrations.[41]

Peaks of PA6 and CA were detected in PA6/CA nanofiber membranes. However, as a result of the interaction of the chemical structures in PA6 and CA, some shifts in the wavelengths of the peaks and changes in the transmittance values of some of them were observed. It has been observed that the peak values in the FTIR spectrum of PA6/CA nanofiber membranes are fully consistent with the literature.

3.2.2. Scanning electron microscopy (SEM) analysis

SEM images of produced PA6/CA-based nanofiber membrane samples and fiber diameter distribution obtained from SEM images are given in Figure 10.

DOI: http://dx.doi.org/10.32571/ijct.1207544 E-ISSN: 2602-277X

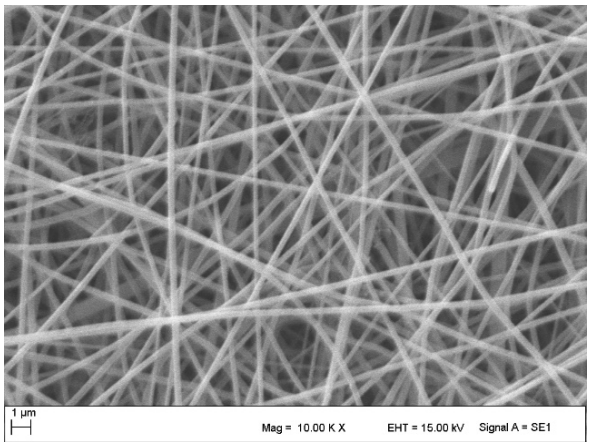

a

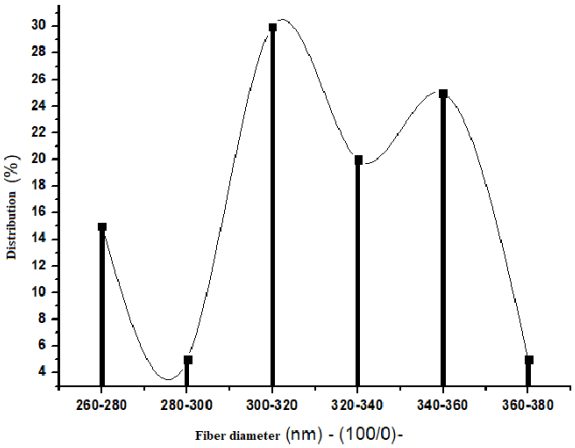

a-1

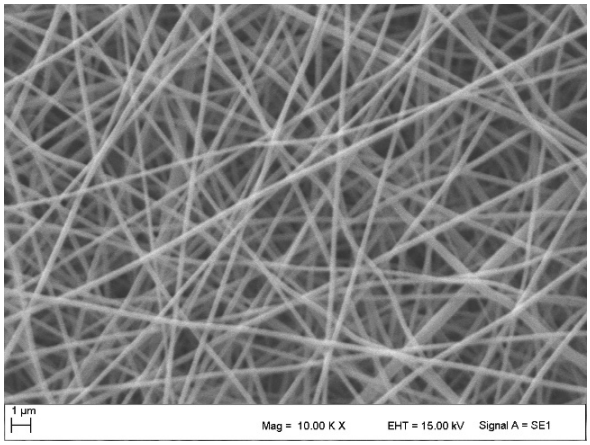

b

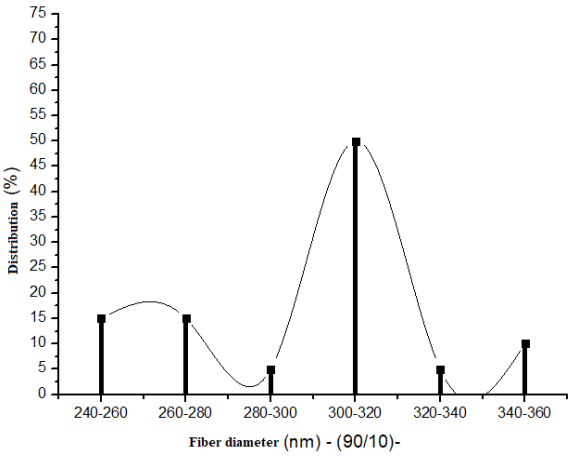

b-1

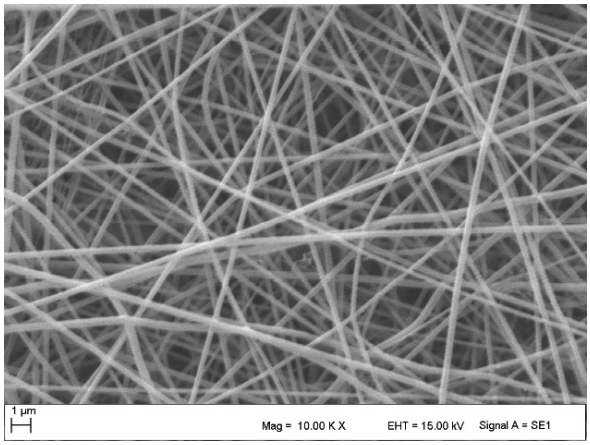

c

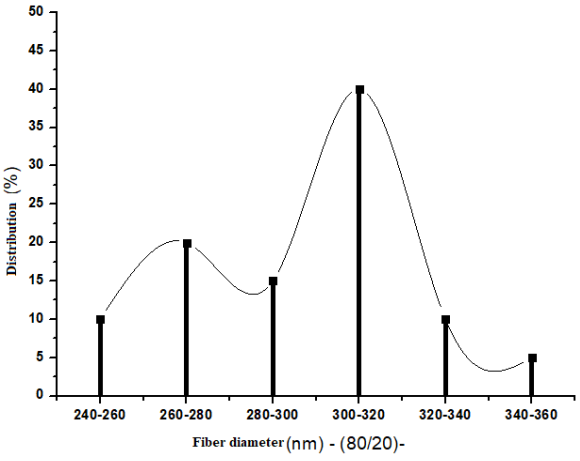

c-1

DOI: http://dx.doi.org/10.32571/ijct.1207544 E-ISSN: 2602-277X

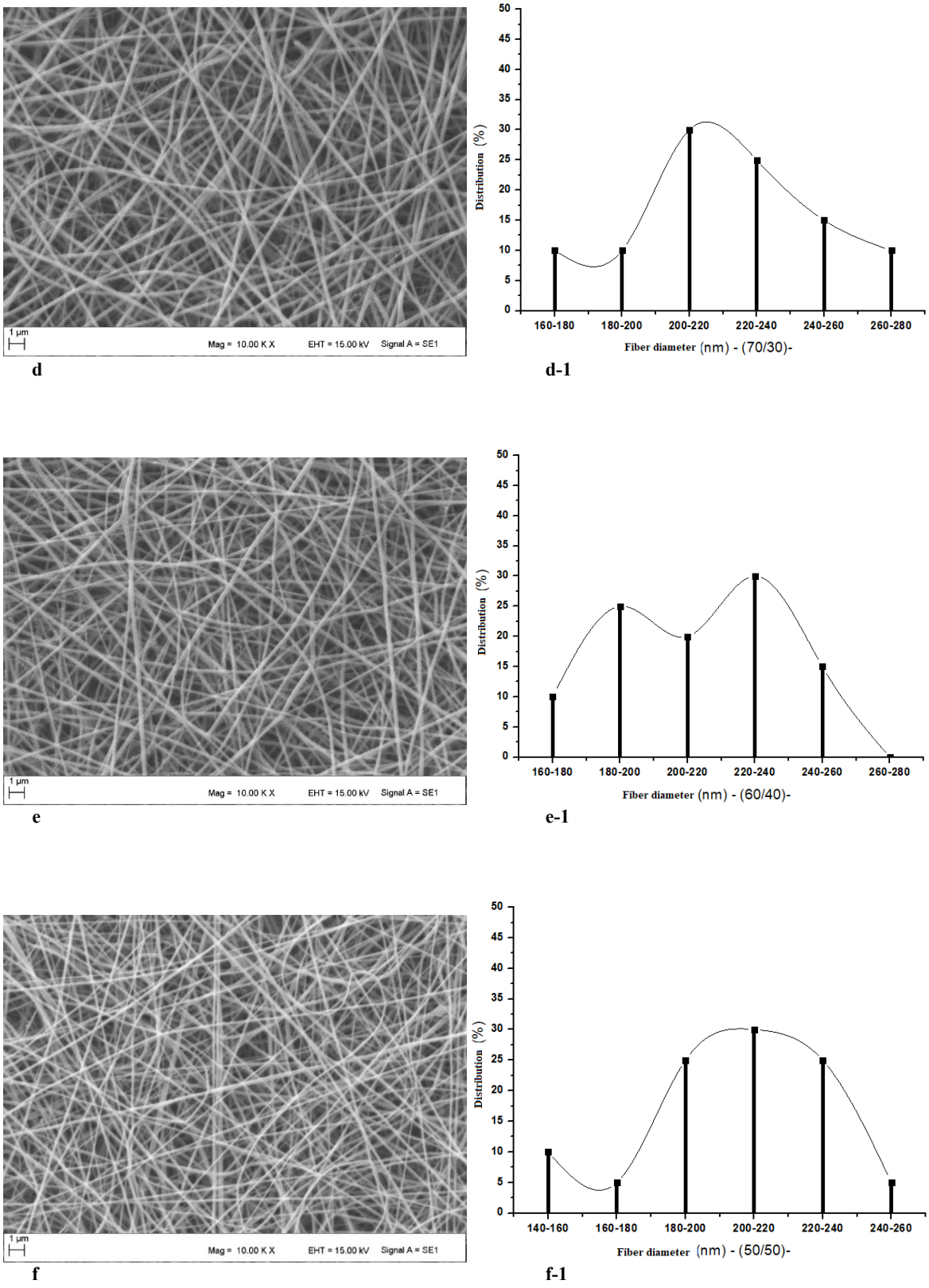

Figure 10. SEM images of nanofiber materials (10 kX) produced by electrospinning method, respectively; a:100/0, b:90/10, c:80/20, d:70/30, e:60/40, f:50/50 and fiber diameter distributions, respectively; a-1:100/0, b-1:90/10, c-1:80/20, d-1:70/30, e-1:60/40, f-1:50/50.

DOI: http://dx.doi.org/10.32571/ijct.1207544 E-ISSN: 2602-277X

When the morphological structure of nanofibers obtained from SEM images is examined, nanofiber structures are clearly seen in general. The absence of the bead structure in these images indicates that a suitable viscosity value for the electrospinning process has been achieved. Thus, it shows that a uniform nanofiber structure is formed for all samples.In addition, the graph of average fiber diameter values of 20 different measurements obtained from SEM images of PA6/CA nanofiber membranes prepared at different mixing ratios is given in Figure 11.

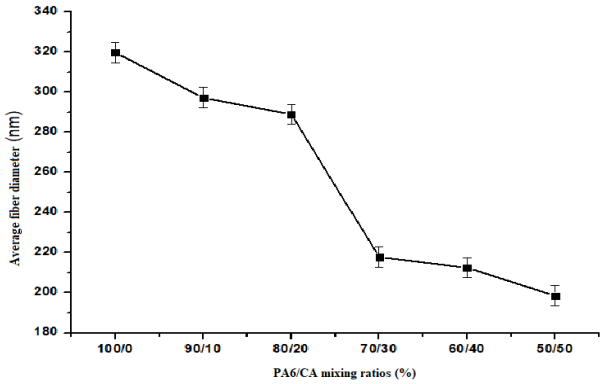

Figure 11. Measured fiber diameter graph of PA6/CA nanofiber membranes at different mixing ratios.

As can be seen in Figure 11, the diameters of the nano-structured membrane fiber can differ with the change in the mass ratios of the PA6 and CA components. In the average fiber diameter evaluation made over the CA mixture ratio, it is seen that the sample with the thinnest average fiber diameters is the sample with 50/50 ratio.

3.2.3. Membrane thickness analysis

The change graph of the membrane thickness values increasing depending on the PA6/CA ratios in different mixing ratios of the membrane structures obtained in nanostructure is shared in Figure 12.

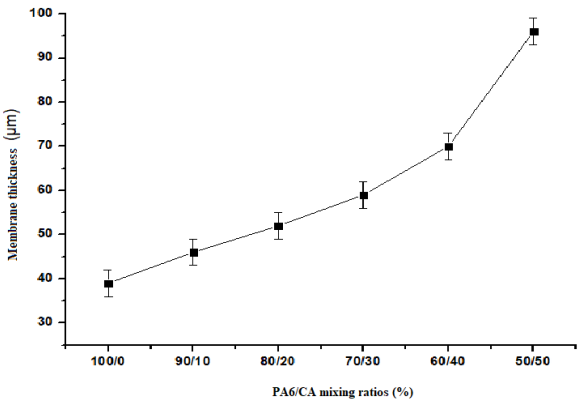

Figure 12. Membrane thickness graph of PA6/CA nanofiber membranes with different mixing ratios.

As seen in Figure 12, it is observed that the thickness measurement values of the obtained membranes increase as the amount of cellulose acetate increases.

It was observed that the obtained membrane thickness values increased with the increase of the CA ratio in the solution with different mixing ratios. It has been determined that these results have produced parallel results with the results in the literature.[42]

3.2.4. Membrane strength properties

The graphs of the membrane mechanical tests for each sample performed depending on the increasing CA ratio in the PA6/CA mixing ratios are in Figure 13, the Young's modulus graph in Figure 14, the elongation graph in Figure 15 and the tensile strength graph in Figure 16. has also been presented.

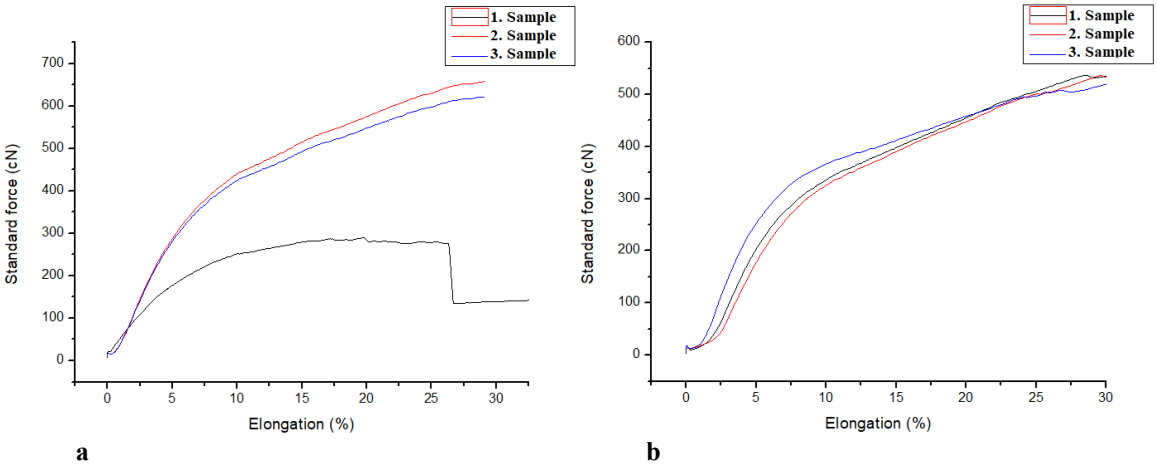

DOI: http://dx.doi.org/10.32571/ijct.1207544 E-ISSN: 2602-277X

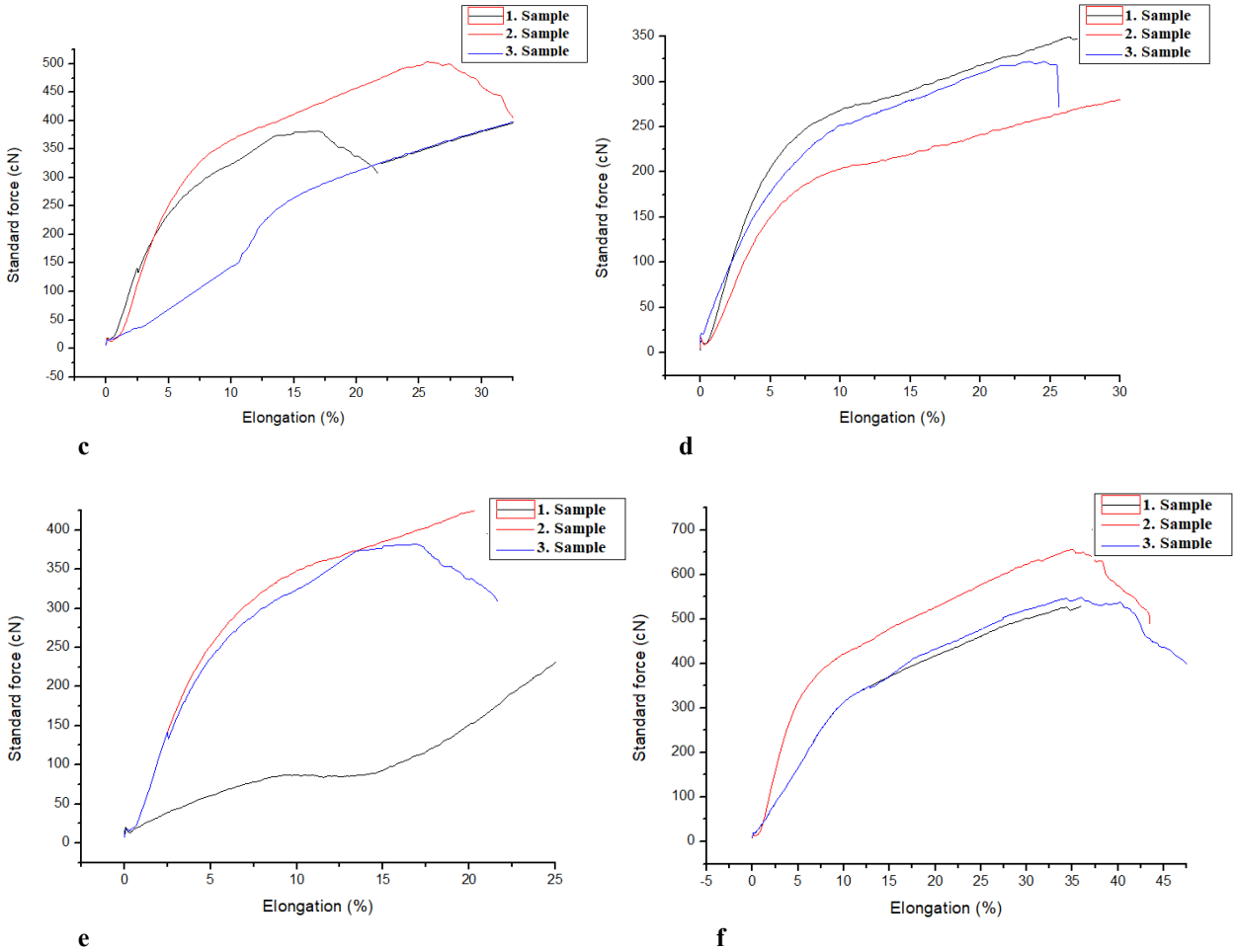

Figure 13. Tensile strength graphs of PA6/CA membranes at different mixing ratios:(a:50-50, b:60-40, c:70-30, d:80-20, e:90-10, f:100-0).

When the changes in the mechanical properties of the nano-structured membranes were examined with the increase in the ratio of the CA amount in the PA6/CA mixtures, it was observed that the Young's modulus in general increased with the increase in the CA ratio.

The result obtained as a result of this observation is compatible with the literature, and Huang et al. attributed this to the formation of high cohesion forces due to the decrease in average fiber diameter.[43] In addition, in another literature study, it was stated that the strength of the nanofibers in the membrane structure increased with the decrease in diameter.[44]

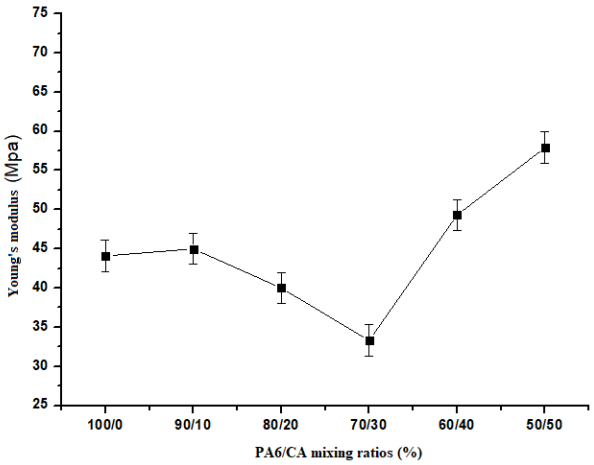

Figure 14. Young's modulus plot of PA6/CA membranes at different mixing ratios.

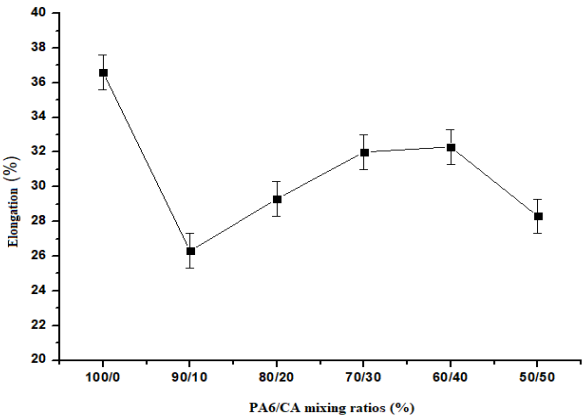

Figure 15. Elongation plot of PA6/CA membranes at different mixing ratios.

DOI: http://dx.doi.org/10.32571/ijct.1207544 E-ISSN: 2602-277X

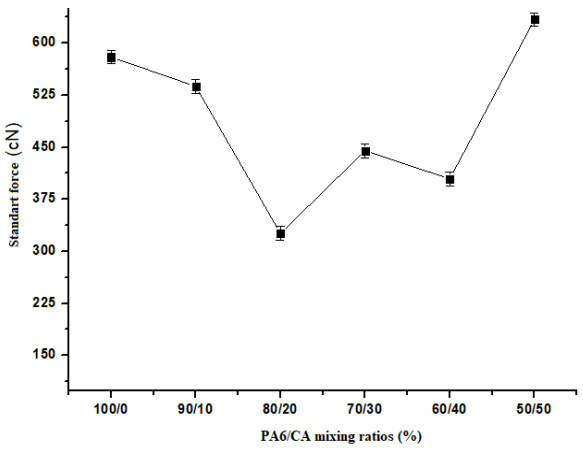

Figure 16. Standard force graph of PA6/CA membranes at different mixing ratios.

4. CONCLUSION

In the study, polymer solutions were prepared from PA6/CA mixtures (100/0, 90/10, 80/20, 70/30, 60/40, 50/50) to produce nanofiber surfaces to be used as filter membranes. The most suitable electrospinning parameters for the production of nanofibers were determined to produce from prepared PA6/CA polymer solutions. Using these parameters, the production of nanofiber surfaces by electrospinning method has been carried out successfully. From the characteristic peak bands obtained as a result of the FTIR analysis, it was determined that the PA6/CA structure was intact in the nanofiber material. In addition, it was determined that smooth and very fine nanofibers were formed in the materials produced from SEM images. It was observed that the conductivity of the solution decreased with the increase of the CA mixing ratio in the PA6/CA polymer solution and accordingly the fiber diameter became thinner. Accordingly, it was concluded that the mechanical properties of the membrane generally increased with the increase in the weight ratio of CA. The results show that these nanofiber surfaces can be used as new membrane materials for industrial applications.

ACKNOWLEDGEMENTS

This study was supported by Kahramanmaras Sütçü İmam University BAP (Scientific Research Projects) unit with project number 2019/1-21D and the 100/2000 PhD scholarship awarded by YÖK (Council of Higher Education) in the field of smart materials.

Conflict of interest

Authors declare that there is no a conflict of interest with any person, institute, company, etc.

REFERENCES

1. Teo, W.E.; Ramakrishna, S. *Nanotechnology*. **2006,** 17(2), 89-106.

2. Gipson, P.; Schreuder-Gibson, H.; Rivin, D. *Nanofibers, Colloids and Surfaces A: Physicochemical and Engineering Aspects*. **2001**, 187/188, 469–481.

3. Lee, K.; Lee, B.; Kim, C.; Kim, H.; Kim, K.; Nah, C. *Macromolecular Research*. **2005**, 13, 441-445.

4. Pedicini, A.; Farris, R.J. *Polymer.* **2003**, 44, 6857-6862.

5. Çetin, E.; Tiyek, İ. *Journal of the Faculty of Engineering and Architecture of Gazi University*, **2021**, 36(4), 1893-1908.

6. Kılıç, A.; Oruç, F.; Demir, A. *Textile Res. J.* **2008**, 78(6), 532–539.

7. Formhals, A. Process and Apparatus for Preparing Artificial Threads. U.S. Patent 1,975,**504**. 1934.

8. Danwanichakul, P.; Danwanichakul. D.; Sueviriyapan, N.; Sumruan, B. Nylon 6/Chitosan Nanofibrous Structures for Filtration, In Proceedings of the 1st Mae Fah Luang University International Conference, **2012**, 1-18.

9. Kozanoğlu, G.S. Elektrospinning Yöntemiyle Nanolif Üretim Teknolojisi. Masters Thesis İstanbul Technical University, İstanbul, **2006.**

10. Tiyek, İ.; Gündüz, A.; Yalçınkaya, F.; Chaloupek, J. *Journal of Nanoscience and Nanotechnology.* **2019**, 19, 7251-7260.

11. Deitzel, J.; Kleinmeyer, J.; Harris, D.; Tan, N. *Polymer*. **2001**, 42, 261-272.

12. Yener, F.; Jırsak, O.; Yalçınkaya, B. *Tekstil Tekn. Elekt. Derg.* **2011**.5(2), 26-34.

13. Nirmala, R.; Nam, K.; Soo-Jin, P.; Yu-Shik, S.; Hak, Y.; Kim, H.; Navamathavan, R. *App. Surface Sci.* **2010**, 256: 6318–6323.

14. Nylon 6. wikipedia.org. https://en.wikipedia.org/wiki/Nylon_6. (accessed October 20, **2022**).

15. Kırcı, H.; Ateş, S.; Akgül, M.. *Fen ve Mühendislik Derg.* **2001**, 4(2), 119-130.

16. Ott, E.; Grafflin, M. *Adgewandte Chem.*, **1956**, 68(14), 471.

17. Saleema, H.; Kılıç, A.; Zaidi, S.J. Desalination, **2020**, 478(2020) 1-40.

DOI: http://dx.doi.org/10.32571/ijct.1207544 E-ISSN: 2602-277X

18. Aslan, M. *Membran Teknolojileri*, T.C. Çevre ve Şehircilik Bakanlığı, TUÇEV Türkiye Çevre Koruma Vakfı Yayınları. Ankara, **2016**.

19. Li, L.; Bellan, L.M.; Craighead, H.G.; Frey, M.W. *Polymer.* **2006**, 47, 6208-6217.

20. Li, Q.; Wei, Q.; Wu, N.; Cai, Y.; Gao. W. *J. App. Poly. Sci.* **2008**, 107, 3535–3540.

21. Polat, Y.; Çalışır, M.; Gungor, M.; Sagirli, M.N.; Atakan, R.; Akgul,, Y.; Demir, A.; Kılıç, A. *J. Ind. Text.* **2021**, 51(5), 821-834.

22. Lee, K.H.; Kim, K.W.; Pesapane, A., Kim, H.Y.; Rabolt, J.F. *Macromolecules*. **2008**, 41(4), 1494-1498.

23. Sivakumar, M.; Mohan, D.R.; Rangarajan, R.; J. Memb. Sci. **2006**, 268(2), 208-219.

24. Jayalakshmi, A.; Rajesh, S.; Mohan, D. App. Surf. Sci. **2012**, 258(24), 9770-9781.

25. Shashidhara, G.M.; Guruprasad, K.H.; Varadarajulu, A. *European Poly. J.* **2002**, 38, 611–614.

26. Joshi, M.K.; Tiwari, A.P.; Maharjan, B.; Won, K.S.; Kim, H.J.; Park, C.H.; Kim, C.S. *Carbohydrate Poly.* **2016**, 147, 104-113.

27. Liaoa, N.; Unnithana, A.R.; Joshi, M.K.; Tiwari, A.P.; Hong, S.T.; Parka, C.H.; Kim, C.S. *Kolloidler ve Yüzeyler A: Fizikokimyasal ve Mühendislik Yönleri*. **2015**, 469(1), 194-201.

28. Khaparde, D. *Carbohydrate Poly.* **2017**, 173(1), 338-343.

29. Mindivan, F. *Machines Tech. Mat.* **2016**, 10(11), 56-59.

30. Lee, K.H.; Kim, K.W.; Pesapane, A.; Kim, H.Y.; Rabolt, J.F. *Macromolecules*, **2008**, 41(4), 1494-1498.

31. Kherroub, D.E.; Belbachir, M.; Lamouri, S.; Bouhadjar, L.; Chikh, K. *Oriental J. Chem.* **2013**, 29(4), 1429.

32. Schneider, B.; Schmidt, P.; Wichterle, O. *Collection of Czechoslovak Chem. Com.* **1962**, 27(8), 1749-1759.

33. Meşeli, H. Alifatik Naylon 6 Liflerinin Karbon Lif Üretiminde Hammadde Olarak Değerlendirilmesi ve Karakterize Edilmesi. Masters Thesis Kayseri Erciyes University, Kayseri, **2014**.

34. Karacan, I.; Meşeli, H. *J. Indust. Text.* **2018**, 47(6), 1185-1211.

35. Sudiarti, T.; Wahyuningrum, D.; Bundjali, B.; Arcana, I.M. *Materials Sci. Eng.* **2016**, 223, 120.

36. Song, J.; Liu, M.; Yang, Z.; Xu, S.; Cheng, B.; Fei, P. *e-Polymers*. **2017**, 17(4), 333-340.

37. Hassan, H.S.; Elkady, M.F.; Farghali, A.A.; Salem, A.M.; Abd El-Hamid, A.I. *J. Taiwan Inst. Chem. Eng.* **2016**, 78, 307–316.

38. Cao, Y.; Wu, J.; Meng, T.; Zhang, J.; He, J.; Li, H.; Zhang, Y. *Carbohydrate Poly.* **2007**, 69, 665-672.

39. He, X. *Membranes*. **2017**, 7(27), 1-9.

40. Fei, P.; Liao, L.; Chen, B.; Song, J. *Analytical Methods*. **2017**, 9, 6194-6201.

41. Selvakumar, M.; Bhat, D.K. *J. App. Poly. Sci.* **2008**, 110, 594–602.

42. Chattopadhyay, S.; Hatton, T.A.; Rutledge, G.C.; *J. Mat. Sci.* **2016**, 51(1), 204-217.

43. Huang, L.; McCutcheon, J.R. *J. Memb. Sci.* **2014**, 457, 162-169.

44. Baji, A.; Mai, Y.W.; Wong, S.C.; Abtahi, M.; Chen, P. *Comp. Sci. and Tech.* **2010**,70(5), 703-718.